Interannual to Multidecadal Timescale Climate Variations in the Northeast Pacific

DANIEL M. WARE

Pacific Biological Station, Nanaimo, British Columbia, Canada

RICHARD E. THOMSON

Institute of Ocean Sciences, Sidney, British Columbia, Canada

(Manuscript received 23 October 1998, in final form 7 December 1999)

ABSTRACT

Analysis of five, long-term coastal air temperature records, reconstructed from tree ring growth patterns, indicate that the climate of the northeast Pacific Ocean has oscillated at three dominant timescales over the last 400 years: the well-known 2–8-yr El Niño–Southern Oscillation (ENSO) timescale, a 20–40-yr interdecadal timescale, and a 60–80-yr multidecadal timescale. The latter oscillation has been the dominant mode of air temperature variability along the west coast of North America over the last 400 years. During this period, there have been conspicuous temporal modulations of the ENSO and the interdecadal signals. Low-frequency temperature oscillations at periods greater than 10 years in the northeast Pacific have been significantly coherent and in-phase from southern California to British Columbia. However, with the exception of the ENSO signal, higher-frequency variability has been weakly coherent along the west coast. Recent work suggests that the interdecadal oscillation is a worldwide phenomenon that relies on global-scale air–sea interactions to explain its existence. Superimposed on this global pattern are basin-scale interactions that force regional variability in ocean climate.

1. Introduction

Variations in global climate occur over a broad range of timescales. Climate variability at any fixed location can be devolved into a series of time-dependent processes comprised of trends, periodic oscillations, and random fluctuations. With the possible exception of the anthropogenic greenhouse gas forcing of global and regional temperatures (a largely twentieth-century phenomenon), long-term trends likely represent low-frequency components that cannot be resolved by the finite length of the instrument time series. Periodic variations are associated with deterministic geophysical processes in the climate system, while random variations are linked to stochastic processes in the system. Climate variability in the northeast Pacific is controlled, to a large extent, by the shifting position of the atmospheric jet stream. The jet stream determines the positions of the high and low pressure systems around which blow the large-scale surface winds. As a consequence, much of the regional climate variation in the northeast Pacific arises during winter when the variability of the jet stream is greatest (Roden 1989).

The climate of the northeast Pacific is also affected by the El Niño–Southern Oscillation (ENSO) phenomenon. Formed through internal oscillations of the tropical ocean–atmosphere system (Rasmusson et al. 1995), ENSO events have occurred with an average return interval of 2–8 yr in the tropical Pacific. Part of the ENSO signal generated in the equatorial Pacific is propagated poleward through atmospheric teleconnections. These events can lead to a deepening of the Aleutian low pressure system, which advects warm, moist subtropical air toward the west coast of North America in winter. Because the resulting warming and increase in rainfall depend on the latitude of the storm tracks and the proximity of the low pressure systems to the coast (Roden 1989; Ebbesmeyer et al. 1991), not all ENSO events produce the same effect. Part of an ENSO event also is propagated to higher latitudes as coastal-trapped, internal Kelvin waves that originate from the eastern equatorial Pacific. These waves induce transient changes in the thermal structure and current patterns in the coastal ocean.

Observations of air temperature and sea surface temperature (SST) from most existing sites along the west coast of North America began about 100 years ago. Longer records (circa 150 years) are available for only

Corresponding author address: Daniel Ware, Department of Fisheries and Oceans, Pacific Biological Station, Nanaimo, BC V9R 5K6 Canada.
E-mail: wared@dfo-mpo.gc.ca

a few scattered sites. Fluctuations in air and surface ocean temperature are strongly correlated at exposed coastal stations (Roden 1989). Both records capture the episodic El Niño signal and the more periodic oscillations at interdecadal timescales (e.g., Roden 1989; Royer 1989; Ware 1995; Minobe 1997; Mantua et al. 1997). Other data sources are needed to resolve longer timescales of temperature variability. High-resolution reconstructions of climate variability spanning the last four hundred to several thousand years have been derived from tree ring growth patterns. By carefully selecting and collecting samples from many trees in homogeneous, climate-stressed sites, ring-width measurements can be averaged and transformed to reveal the common regional climate signal (Fritts 1991). Michaelsen (1989), for example, used records of tree ring widths from the southwest United States and northwest Mexico to reconstruct a 400-yr El Niño time series. By calculating sequential ''evolutive'' power spectrum for these time series, Michaelsen determined how the amplitude and frequency of the El Niño signal has evolved over time. He found that the amplitude and frequency of El Niño events have been modulated over an 80–100-yr period. Significant variability also occurs at interdecadal and multidecadal timescales, producing climate regimes that last for 20–30 yr (Ware 1995; Minobe 1997). These changes have a large and persistent impact on marine fisheries and the ecosystems that support them. For example, Ware and Thomson (1991) found evidence for multidecadal oscillations in wind-induced upwelling and the productivity of Pacific sardine and hake in the California Current system. If history repeats itself, future climate regime changes of this kind are likely to have significant societal impacts on the industrial and recreational marine fisheries in the northeast Pacific.

The purpose of this study is to examine reconstructed air temperature time series for the west coast of North America for the past 400 years in order to: 1) determine the dominant timescales of ENSO events, and interdecadal oscillations in the northeast Pacific; 2) identify the time-dependent frequency and amplitude modulations that have occurred over these timescales; and 3) delineate the north–south structure for the resulting dominant modes of climate variability. Some possible causes for this low-frequency variability suggested by recent empirical analyses and climate general circulation models (CGCMs) simulations are discussed.

2. Data source

Dendrochronological studies of climate variation are based on annual incremental growth patterns in the wood stem of trees exposed to marked seasonal changes in temperature, rainfall, and other growth-modifying factors. In the warm regions of southwestern North America, low precipitation and high temperatures during the growing season are linked to the formation of narrow rings in arid-site trees. For example, a narrow ring is the result of low soil moisture and increased evaporation, which lead to increased water stress in the tree (Douglas 1980). To dervive a reconstructed temperature record, the raw tree ring width data are subjected to a complex standardization, filtering, and verification analysis. Standardization permits tree-to-tree comparisons by removing the effects of age and size, and by normalizing the amplitudes of the individual tree ring time series to a common level of variance. The resulting standardized time series are then transformed into reconstructed climate time series using principal components and multiple linear regression models (Fritts 1991).

The air temperature time series (1602–1961) used in this study were obtained from the National Geophysical Data Center, Boulder, Colorado (available online from ftp://ftp.ngdc.noaa.gov), and were last updated by Fritts in 1991. Briefly, Fritts calibrated the tree ring data with climate data for the 1901–63 period, verified the calibration against all available climatic data prior to 1901, and combined the results of the best two to three reconstructions (from models of different structure) to produce the final air temperature reconstructions. The reconstructed time series (T_i) are stored as anomalies (°C), $T_i = (X_i - X)$, where X_i is the original data in the ith year, and X is the mean of the record for the calibration period.

Since we were interested in analyzing proxy records of coastal SST, we selected five sites from Fritts' database that were closest to the west coast of North America (Fig. 1): Visalia, Sacramento, and Eureka, California; Aberdeen, Washington; and Vancouver, British Columbia. Previous work has shown that coastal air temperatures tend to be linearly correlated with local SST at a high level of significance (e.g., Roden 1989; Ware 1995).

We tested the accuracy of Fritts' air temperature reconstructions by examining their correlation with instrument air temperature measurements from nearby coastal weather stations (obtained from the PACLIM database, Cayan et al. 1991). Over the 62–84-yr period of overlap in the five records, Fritts' reconstructed temperature anomalies for each site were found to be highly correlated with annual air temperature anomalies at nearby weather stations (Table 1). These tests confirmed that Fritts' time series provided an acceptable description of average temperatures at the five reconstruction sites. To obtain the longest possible records at each site, we used our site-specific linear regressions, which related Fritts' reconstructed air temperature (dependent variable) to the measured temperature anomalies (independent variable) at the weather stations listed in Table 1. The resulting estimates of the dependent variable (for the years 1962–84) were then appended to Fritts' reconstructed time series to extend the records an additional 23 yr at each site. These extended time series were then standardized (so they had a zero mean and unit standard deviation) by dividing the reconstructed

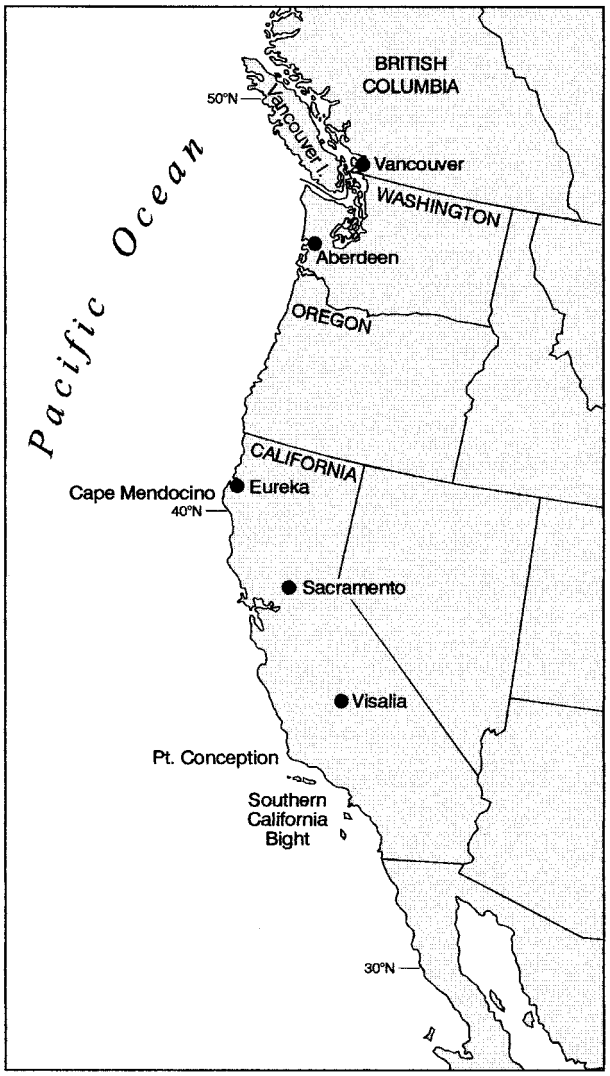

FIG. 1. Locations of the five tree ring sites (indicated by dots) near the west coast of North America where coastal air temperature anomalies have been reconstructed from 1602 to 1984.

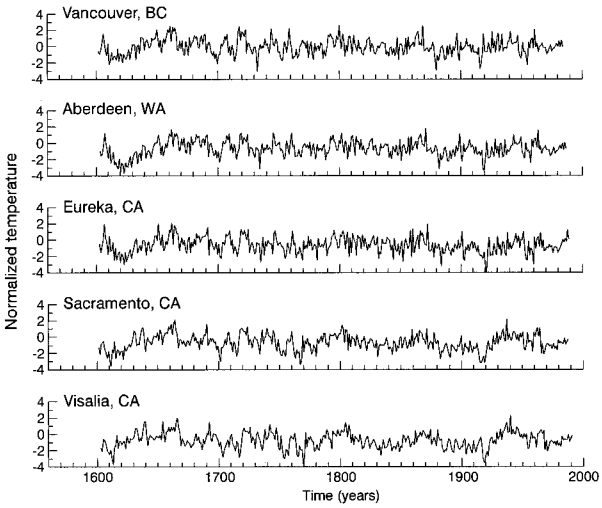

FIG. 2. Annual coastal air temperature anomaly time series (expressed in standard deviation units) for the five tree ring sites shown in Fig. 1. The chronology at each site is based on an average of at least two replicated core samples from 10 to 30 trees. Adapted from Fritts (1991).

annual estimates by the standard deviation of the extended 383-yr time series. Accordingly, the air temperature time series used in this paper are in standard deviation units (Fig. 2).

As indicated by the integral timescales shown in Fig. 3, the tree ring records for all sites consist of high-frequency temperature variations with decorrelation times of 2–4 yr superimposed on much lower-frequency variations with timescales of many decades. The integral timescale, $T = 1/R(0) \int_0^\infty R(\xi)\, d\xi$, is a statistical measure of the characteristic timescale for each reconstructed temperature record based on its autocorrelation function, $R(\xi)$, for time lag ξ (Emery and Thomson 1998). The pronounced sinusoidal-type variations in the integral timescales for Sacramento and Visalia suggest that low-frequency temperature variability is especially persistent at the more southern sites in the study region.

3. Extreme warm and cool anomalies and past climate regimes

The reconstructed records (Fig. 2) were examined to identify the coolest and warmest years along the west coast of North America in each century (Table 2). The results indicate that extreme warm and cool spells occurred simultaneously at the northern and southern ends

TABLE 1. Locations of the reconstructed air temperature time series and nearby weather stations used to test the accuracy of Fritts' reconstructions. The last column shows the correlation between the annual air temperature anomalies at the reconstruction site and the weather station site, the number of years of overlap in the two time series (n), and the significance of the correlation.

Reconstruction site	Location (°N latitude)	Weather station	Correlation coefficient
1. Vancouver, BC	49.2	Gonzales, BC	0.66; $n = 62$; $p < 0.001$
2. Aberdeen, WA	46.6	Gonzales, BC	0.66; $n = 62$; $p < 0.001$
3. Eureka, CA	40.5	Eureka, CA	0.59; $n = 75$; $p < 0.001$
4. Sacramento, CA	38.3	Los Angeles, CA	0.67; $n = 84$; $p < 0.001$
5. Visalia, CA	36.2	Los Angeles, CA	0.69; $n = 84$; $p < 0.001$

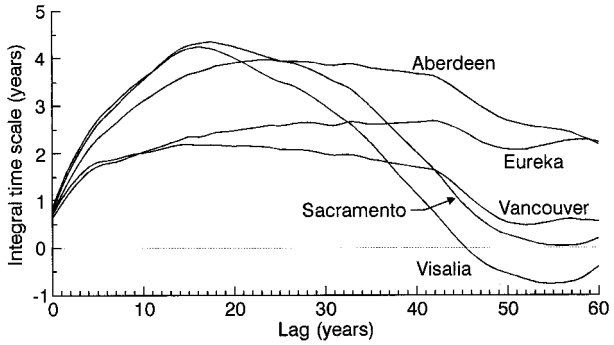

FIG. 3. Integral timescale plots for the five time series. The peaks in the curves for each site indicate that the decorrelation timescale is about 2–4 years. The sinusoidal-type curves for Sacramento and Visalia suggest that low-frequency variability is persistent in the southern part of the study region.

of the study area. The coolest anomalies occurred in the Vancouver record between 1879 and 1883, and in the Sacramento record between 1911 and 1917. Coastal air temperature instrument records for New Westminster, British Columbia; and Eureka, San Francisco, Los Angeles, and San Diego, California (Cayan et al. 1991) confirm that the interval between 1907 and 1917 was indeed cold (with the exception of 1914 and 1915 in British Columbia.). The warmest anomalies occurred in both the Vancouver and Sacramento records between 1656 and 1666. The two most recent warm anomalies in these records (1939–43 and 1958–61) were both associated with strong ENSO events.

Analyses of twentieth-century sea level pressure (SLP) and temperature time series measurements indicate the presence of abrupt interdecadal climate regime shifts (e.g., Ware 1995; Minobe 1997). Climate regimes are defined as climate anomalies that tend to have the same sign for a decade or more. Minobe (1997) identified climate regime shifts in spring air temperature and coastal SST in the 1890s, 1920s, 1940s, and 1970s for western North America. The reconstructed temperature records examined here also indicate the presence of large regime shifts in the past. In our analysis, a regime shift was considered to have occurred when the sign of the temperature anomalies changed from the previous state for at least 3 years. This criteria was adopted to allow for the fact that high-frequency variability, such as a strong El Niño (La Niña) event, can punctuate a cool (warm) regime and cause a temporary change in sign for a year or two. The duration of past regimes and the approximate timing of regime shifts in the Sacramento temperature record are shown in Table 3. The results indicate that cool regimes in southern California have lasted an average of 26 years and warm regimes about 32 years. In general, we found that the duration of the regimes (Table 3) were in broad agreement with coastal California SST records reconstructed by Douglas (1980), and with directly measured coastal air temperature records assembled by Cayan et al. (1991), begin-

TABLE 3. Duration of warm and cool climate regimes in the reconstructed air temperature record for Sacramento (mean ± standard error). These results suggest that major climate regime changes off California occurred around 1630, 1696, 1717, 1746, 1755, 1761, 1782, 1826, 1855, 1879, 1923, 1945, and 1976.

Cool phase	Warm phase
?–1629	1630–95 (66)
1696–1716 (21)	1717–45 (29)
1746–54 (9)	1755–60 (6)
1761–81 (21)	1782–1825 (44)
1826–54 (29)	1855–78 (24)[a]
1879–1922 (44)[b]	1923–44 (22)[c]
1945–75 (31)[d]	1976–?
Average cool period duration	Average warm period duration
25.8 ± 4.8 yr	31.8 ± 8.5 yr

[a] Instrumented air temperature (IAT) records indicate that the 1855–78 warm regime began in 1852 and ended in 1872 around San Diego. The IAT records are from Cayan et al. (1991).

[b] IAT records for San Francisco, Los Angeles, and San Diego place the end of this regime in 1922.

[c] The implied end of this regime in 1944 is consistent with IAT records for San Francisco and Eureka.

[d] The duration of this regime was determined from sea surface temperature anomalies at La Jolla, Southern California (Schwing 1994).

TABLE 2. Extreme cool and warm spells between 1602 and 1961 in the Vancouver and Sacramento reconstructed air temperature records. The average temperature anomalies (in standard deviations) for these periods are shown in brackets.

Vancouver cool	Sacramento cool	Vancouver warm	Sacramento warm
1609–19 (−1.18)	1608–14 (−1.63)	1658–66 (+1.81)	1656–66 (+1.64)
1695–02 (−1.10)	1698–03 (−1.04)	1717–23 (+1.68)	1717–23 (+1.52)
1750–54 (−1.18)	1750–54 (−1.38)	1791–95 (+1.27)	1797–01 (+1.37)
1762–67 (−1.10)	1761–67 (−1.62)	1863–69 (+1.15)	1863–65* (+1.28)
1879–83** (−1.65)	1879–83 (−1.17)	1939–42 (+0.90)	1939–43** (+0.99)
1911–18 (−1.11)	1911–17** (−2.03)	1958–61 (+0.93)	1956–61 (+1.28)

* The 1863–65 warm spell (apparent in all five reconstructed records) is consistent with the San Diego instrumented record (which was warm between 1861 and 1868), but not the San Francisco record (which indicates cool conditions at that time). The cooling around San Francisco may have been caused by an intensification of local upwelling.

** The cool 1879–83 and 1911–17 spells, and the warm 1939–43 spell are all consistent with the San Francisco, Los Angeles, and San Diego instrumented air temperature records (Cayan et al. 1991).

ning in the mid- to late 1800s. For reasons unknown, the reconstructed temperature record for Sacramento failed to record the mid-1940s regime change, which is clearly apparent in the La Jolla, California, SST (Schwing 1994), and the Los Angeles air temperature records (Cayan et al. 1991). Our results are consistent with the regime change dates suggested by Minobe (1997), with the exception of the 1879–1922 cool regime, which our reconstructions suggest began about a decade earlier in the northeast Pacific.

4. Spectral and frequency demodulation analyses

We examined the dominant timescales of the reconstructed records using power spectral analysis and wavelet transform methods (Emery and Thomson 1998). Although spectral analysis is best suited to stationary random processes, it remains a well-established tool for processing a wide variety of time series data. The method also allows the user to place confidence intervals on individual spectral peaks, contrary to other frequency domain analysis methods. Wavelet analysis is the best method for examining relatively slow changes in the frequency content of nonstationary time series. Here, ''slow'' refers to the signal modulation timescale τ which is assumed to be long compared to the sampling time t (i.e., $\tau \gg t$). The primary drawback of wavelet methods is the inability to place statistical reliability bounds on spectral amplitudes and phases.

Spectral estimates for each temperature series were obtained as follows. The data series were first padded with zeroes to 512 years, corresponding to 2^N ($N = 9$) data values, for the fast Fourier transform used in the spectral analysis programs. Block averaging of the spectral estimates was used to improve statistical reliability. Specifically, the records were divided into 128-yr blocks with 50% overlap; spectral analysis was applied to each block following the application of a Kaiser–Bessel window. Spectral values for each frequency band were then averaged for the final spectral estimates. Because the window emphasizes the central portion of each data series, each spectral estimate is considered statistically independent, yielding 10 degrees of freedom per spectral band (cf. Emery and Thomson 1998). The gain in statistical reliability provided by the shorter 128-yr data series is offset by an inability to accurately delineate low-frequency variability at periods longer than about 100 years.

Frequency demodulation of the time series was performed using a Morely wavelet transform with 10 cycles. This provided the best trade-off between temporal resolution and frequency resolution. (As with any demodulation algorithm, enhancing the temporal resolution of the demodulated time series degrades the frequency resolution of the time series, and vice versa.) The resulting frequency–time plots reveal how air temperature fluctuations at various timescales change at the slow, signal modulation timescale τ.

5. Spectral time series analysis

There are obvious similarities among the reconstructed temperature time series, particularly at longer timescales, which diminish with increasing separation between locations. Although these records contain both deterministic and random time-varying components, histograms of the reconstructed temperatures at the various sites are not statistically distinguishable from histograms of pseudo-temperature records generated using a Gaussian random number generator. From this perspective, the data are amenable to standard time series analysis procedures.

Power spectral analysis of the reconstructed time series indicates that climate variability in the northeast Pacific occurs at several characteristic timescales (Fig. 4). All sites show evidence for interannual oscillations with a 2–8-yr period associated with the return times of ENSO events in the equatorial Pacific (Aberdeen is similar to Vancouver and is not shown). There also is evidence for interdecadal oscillations with a 20–40-yr period that are probably caused by natural internal oscillations of the North Pacific climate system (Latif and Barnett 1996; Yukimoto et al. 1996; White and Cayan 1998). A broad multidecadal spectral peak was also found at periods of roughly 60–80 years. At the two southern sites, the largest spectral peaks occurred around 70 years, while at the three northern sites there were large spectral peaks around 70 and 130 years. The latter peak was present but not as prominent in the two most southern time series. However, the existence of significant climate variability in the 110–130-yr timescale (which is at the limit of frequency resolution for the 128-yr data blocks used in our spectral analysis) is confirmed by a much longer time series from the nearby Sierra Nevada region (Scuderi 1993).

Rasmusson et al. (1995) provide an SST anomaly record that indicates ENSO cycle variations over the equatorial Pacific from 1874 to 1991. We extracted the peak amplitudes (°C) of the largest ENSO events (where the amplitude exceeded 1.0°C) from their record, and compared them with the reconstructed temperature anomalies at our five west coast of North America sites. Table 4 indicates that ENSO events beginning in 1888, 1902, and 1911 failed to propagate to the west coast of North America. In contrast, the events beginning in 1877, 1896, 1925, 1930, 1941, 1943, and 1957 produced moderate to strong temperature anomalies along the entire west coast. The 1899 and 1905 El Niño events produced moderate to strong temperature anomalies off Washington and British Columbia, but not in Southern California. This suggests that the atmospheric teleconnection, which affects the strength of the Aleutian low pressure system, was not well developed in 1899 and 1905, and that the coastally trapped internal Kelvin wave associated with these two ENSO events failed to propagate from the eastern tropical Pacific to southern California. The opposite situation may have occurred

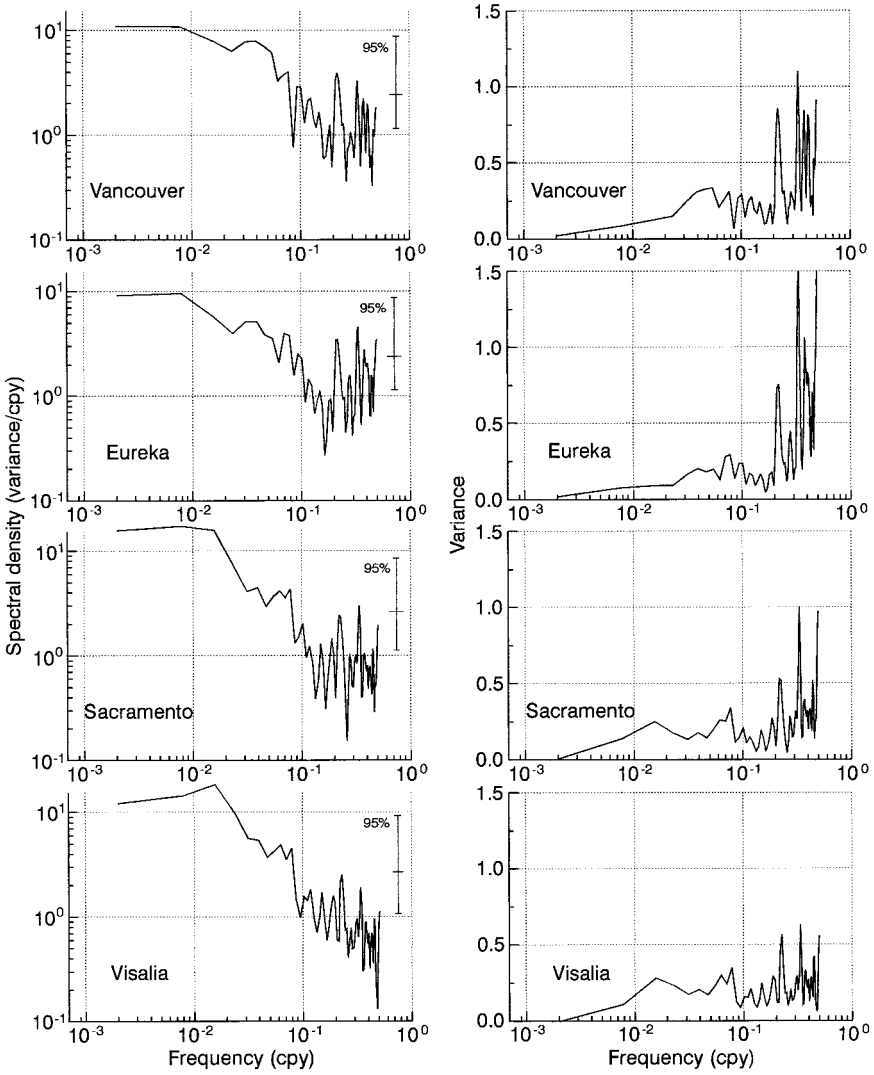

FIG. 4. Power spectra (in standard deviation units) vs frequency (cpy; cycles per year) for the reconstructed time series. The panels on the left indicate the standard power spectra of log spectral density, $\log\phi(f)$, vs log frequency, $\log f$. The panels on the right indicate the signal variance, $f\phi(f)$ vs log frequency. The integral under any segment of the right-hand curves is equal to the variance of the time series in that frequency band. Prominent spectral peaks occur at frequencies (periods) of 0.21 (4.8 yr), 0.06 (17.2 yr), 0.029 (34.8 yr), 0.014 (73 yr), and 0.0078 (128 yr). Each time series has 383 records (padded with zeros to 512 records) and 10 degrees of freedom per spectral estimate. Note that a frequency of 10^{-1} cpy = a 10-yr period and 10^{-2} cpy = 100-yr period.

during the 1952 event, which only produced moderate positive temperature anomalies at the two southern sites. During this event, the atmospheric teleconnection was presumably poorly developed, and the coastally trapped Kelvin waves only travelled as far north as central California.

In addition to the previously noted spatial variability in the strength of El Niño events along the west coast of North America, both the frequency and amplitude of the ENSO cycle appear to be modulated over long timescales. Michaelsen (1989) extracted an ENSO index from seven, 400-yr tree ring width records from New Mexico state and northwestern Mexico. He found that the average period between ENSO events varied between 3 and 8 years, and that both the amplitude and frequency of the ENSO signal were modulated over an 80–100-yr timescale. Using a maximum entropy analysis of overlapping 20-yr segments of the Visalia, California, record, we also found a frequency modulation of the ENSO signal at a timescale of roughly 100 years (Fig. 5). At this southernmost site, the ENSO period was relatively short (about 3 years) around 1732, 1800, and 1892, and relatively long (about 8 years) around 1682, 1870, and 1912. The modulation pattern of the

TABLE 4. Significant ENSO events and their amplitudes (SST anomalies in °C from Rasmusson et al. 1995) in the tropical South Pacific (0°–10°S, 90°W–180°) for the past 100 years, and reconstructed air temperature anomalies (standard deviations) in the five west coast of North America time series. The tabulated values indicate the largest positive (or smallest negative) temperature anomalies recorded at the five reconstruction sites during each 2-yr ENSO event. Some ENSO events produce the largest anomalies in the onset year, others in the second year.

ENSO events	Amplitude	Vancouver	Aberdeen	Eureka	Sacramento	Visalia
1877/78	2.9	+0.55	+0.35	+0.20	+0.29	+0.11
1888/89	2.1	+0.09	−0.29	−0.36	−0.21	−0.04
1896/97	1.6	+1.67	+1.83	+1.65	+0.83	+0.20
1899/00	1.5	+0.57	+0.64	−0.21	−0.02	−0.44
1902/03	1.5	−0.17	+0.14	+0.09	−0.62	−1.15
1905/06	1.7	+1.00	+1.11	+0.44	−0.54	−0.89
1911/12	1.5	−0.66	−0.60	−1.05	−1.24	−0.76
1918/19	1.3	+1.56	+0.94	+0.96	+0.16	+0.39
1925/26	1.1	+1.82	+1.17	+1.05	+1.32	+1.42
1930/31	1.3	+1.67	+0.66	+0.40	+1.65	+2.25
1941/42	1.1	+1.82	+1.73	+1.41	+1.11	+0.97
1943/44	1.6	+0.29	+0.76	+1.11	+0.97	+0.73
1952/53	1.2	−0.60	−0.21	−0.36	+0.25	+0.41
1957/58	1.5	+0.80	+1.21	+0.70	+1.43	+1.16

average ENSO return time between 1875 and 1972 that we obtained (Fig. 5) is similar to the pattern observed in Rasmussen et al.'s (1995) tropical SST record. The latter time series confirms that after 1950 the duration of ENSO events decreased, while their intensity increased.

At our three northern sites (Vancouver, Aberdeen, and Eureka), the temperature time series are all strongly coherent at the 95% level of significance and have nearly zero phase difference at all frequencies (Fig. 6a). This also is true of the coherence between the time series for the two southern sites (Sacramento and Visalia). Our analysis further shows that the low-frequency oscillations (periods greater than 10 years) are mainly coherent and have zero phase shift along the entire coast from

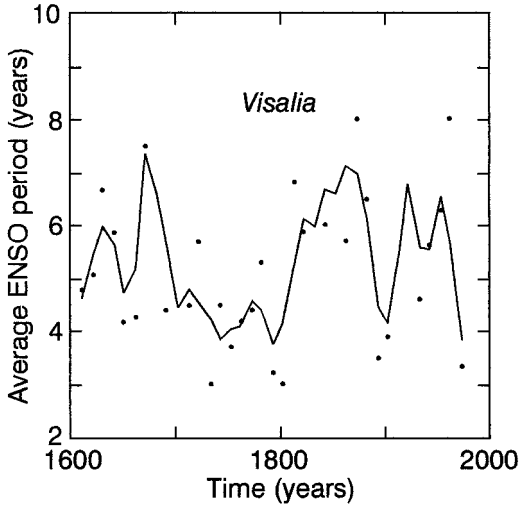

FIG. 5. Average period (yr) of the ENSO cycle determined by maximum entropy analyses of overlapping 20-yr segments of the Visalia time series. The period of this signal appears to be modulated, in a cyclical pattern, at a timescale of about 100 years.

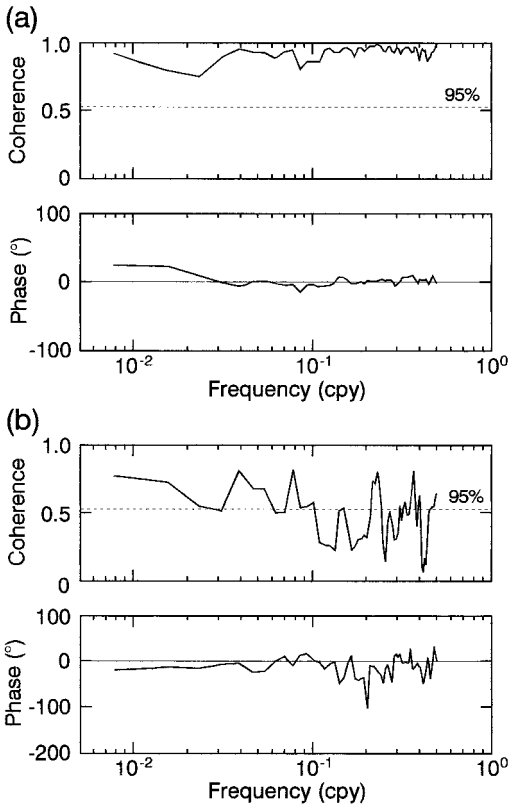

FIG. 6. Spectral coherence between air temperature records for selected sites along the west coast. (a) Vancouver, British Columbia, and Aberdeen, Washington; and (b) Vancouver, British Columbia, and Visalia, California. The top panel in each figure indicates the coherence amplitude (with the 95% confidence level), and the bottom panel the relative phase. Note that a frequency of 10^{-1} cpy = a 10-yr period and 10^{-2} cpy = 100-yr period.

Southern California to southern British Columbia, while high-frequency variability (periods less than 10 years) tend to be noncoherent (Fig. 6b). However, several major exceptions to these generalizations are worth noting. In particular, there is high, coastwide coherence among all locations for air temperature variability in the 2.5-yr and the 5-yr ENSO band, and relatively low coherence between Aberdeen and Visalia in the low-frequency band. The latter finding is problematic (and unexplained) given the much higher coherences between Vancouver and Visalia in the low-frequency band.

6. Wavelet time series analysis

Results of our wavelet analysis in the frequency range 0.01–0.10 cycles per year are shown in Fig. 7. At the two northern sites (Vancouver and Aberdeen), a 70–80-yr signal dominated the beginning of the record, died out by the mid- to late 1700s, then reintensified in the twentieth century. These sites also display a prominent signal at the 20–40-yr timescale. This is consistent with Royer (1989) who found that 20–30-yr interdecadal oscillations in SST were more pronounced above 40°N latitude in the northeast Pacific. In general, the power spectra at Vancouver has evolved much like the Aberdeen spectrum, except for the presence of some higher-frequency components with periods less than 20 years at the Vancouver site.

The demodulated time series for Eureka differs markedly from those for the two southern sites (Fig. 7). At Eureka, the 60–80-yr oscillation has been less well defined and higher-frequency variability more prevalent, particularly during the seventeenth and twentieth centuries. The beginning of the Eureka record was dominated by a strong signal with a roughly 50-yr period. This oscillation died out by the mid-seventeenth century, while a 60–80-yr signal intensified and dominated the record until the late 1800s. As this signal, in turn, weakened, the 50-yr period oscillation reintensified and has dominated the record for most of the twentieth century.

For the Sacramento and Visalia time series, the coastal air temperature variability has been dominated by a strong 60–80-yr period signal, with weak, intermittent oscillations at nominal periods around 15 and 30 years, particularly during the seventeenth, eighteenth, and twentieth centuries (Fig. 7). The nominal 70-yr signal persisted throughout the entire record, with a slight attenuation in the seventeenth century at Visalia. This low-frequency signal was most persistent at Sacramento where it has dominated the air temperature record for the last 400 years (Fig. 7). In general, the demodulated temperature record for Sacramento appears to combine the dominant components of the variability observed at the sites immediately to the north and south. For example, during the late 1700s to early 1900s, the 70-yr oscillation was weak in northern California, Washington, and southern British Columbia, but was strong in Southern California.

Figure 7 indicates that at all five sites, the 60–80-yr signal has undergone a slight amplitude modulation over the last four centuries. In addition, the average period of this signal decreased from about 75 years in the 1600s to 70 years by the early 1800s. Since then, the average period has increased to roughly 75 years. There also has been a time-evolving frequency modulation of the dominant signal in the 10–40-yr band. For example, at Visalia the period of this interdecadal signal declined from 30 to about 13 years between the late 1600s to 1700s, and then seemed to disappear. A reintensified signal in this frequency band appeared in the mid-1800s.

7. Spatial patterns

Empirical orthogonal function (EOF) analysis of the reconstructed air temperature time series for the five sites indicates that there are two principal features in the spatial pattern (Fig. 8). The first mode accounts for 80% of the signal variance and has the same sign (i.e., is positive or negative simultaneously) at all sites. The second mode explains 16% of the variance and changes sign between the three northern sites (Vancouver, Aberdeen, and Eureka) and the two southern sites (Visalia and Sacramento). The transition in sign for mode 2 occurs around 39°N (Fig. 8).

Our mode 1 and 2 spatial structures are similar to those obtained by Cayan (1980), who found that the first EOFs for winter temperature and precipitation were of the same sign along entire west coast of North America, explaining about 67% and 42% of the variance in temperature and precipitation, respectively, between 1934 and 1973. Mode 2 in Cayan's (1980) study accounted for about 17% and 28% of the temperature and precipitation variance, respectively, and had the same sign in the north, and the opposite sign in the south. The mode 2 transition point occurred between 39° and 43°N. Hsieh et al. (1995) reported similar spatial patterns in the winter (and summer) alongshore windstress in the same geographical region during this century. Mode 1 of the windstress, which accounted for 43% of the summer and 45% of the winter variance, had the same sign along the west coast of North America. Mode 2, which accounted for 29% of the summer and 33% of the winter variance, was of one sign for the northern stations (42°–57°N), and of the opposite sign for the southern stations (22°–37°N). The transition in the mode 2 windstress occurred between 40° and 45°N.

These three analyses indicate that the dominant mode of variability for a given variable such as coastal air temperatures, alongshore winter (and summer) windstress, and winter precipitation, cooscillates (i.e., has near-zero phase lag) along the entire west coast of North America. In contrast, the second mode of variability, which accounts for about half the variance of the first mode, has the same sign poleward of latitude 40°N, but

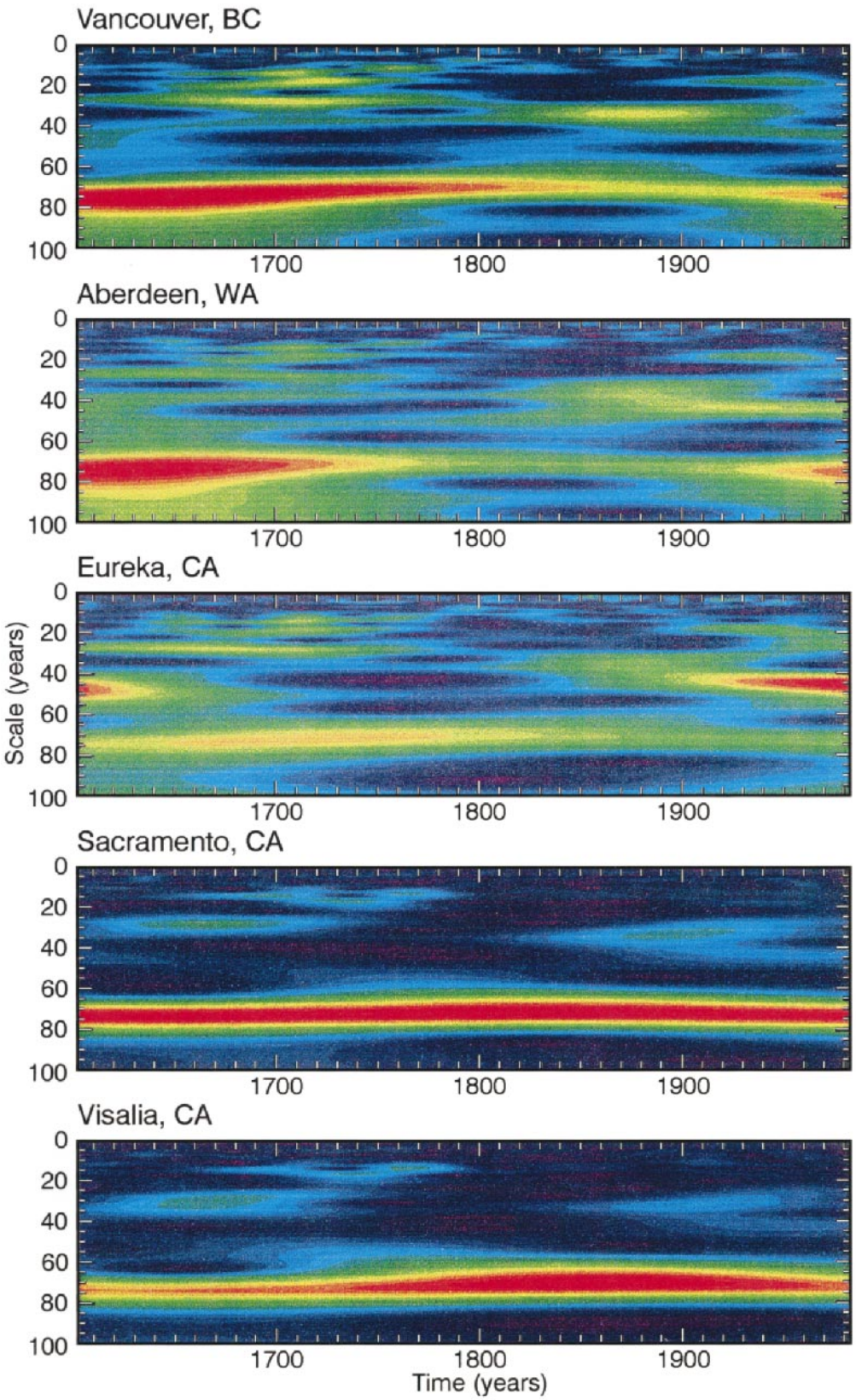

FIG. 7. Wavelet demodulation analysis of the coastal air temperature records for the frequency range 0.01–0.10 cpy (periods of 10–100 years). In each case, we have used a Morley wavelet with 10 cycles. Large signal amplitudes are shown in red and low amplitudes in blue.

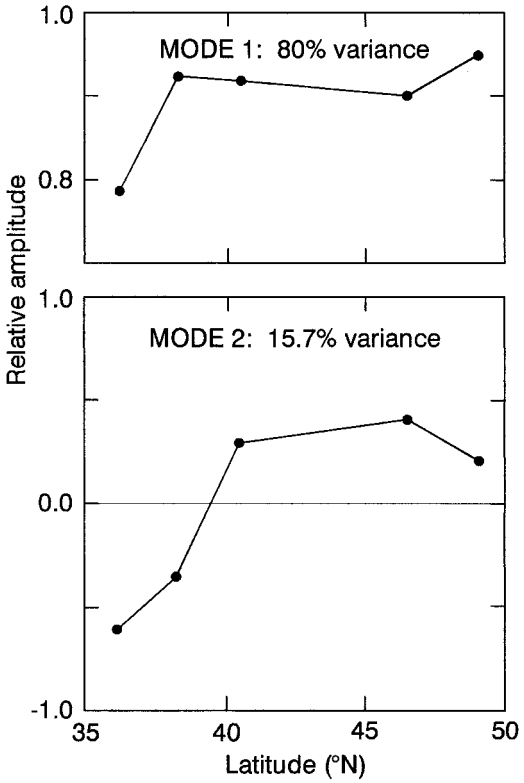

FIG. 8. The first two EOFs for the reconstructed air temperature time series at the five sites. The relative amplitude is the correlation coefficient of each mode with the reconstructed air temperature time series at each site.

the opposite sign at more southern latitudes. For this mode, the northern and southern regions are 180° out of phase. Cayan (1980) suggested that the phase transition between regions probably reflects the position of a northern or southern storm track in the winter period. Similarly, Roden (1989) found that the coherence in air temperature records from northern Washington state to Southern California was high over distances of 600–800 km. Beyond 800 km, the coherence dropped but was still moderately high; beyond 1500 km, the coherence became marginal. Consequently, northeast Pacific coastal air temperatures are coherent over distances of 1500 km, which approximates the diameter of the dominant air pressure systems (Roden 1989).

Demodulation analysis of the mode 1 time series (Fig. 9) indicates the striking prominence of the nominal 60–80-yr signal in the air temperature records. Weakening of this signal in the early 1700s and late 1800s was associated with the appearance of higher-frequency variability at timescales of 10–40 years. Figure 9 also indicates a time-dependent modulation of the 10–40-yr timescale signal in the first half of the record. Around 1600 this signal had an average period of roughly 30 years; by the mid-1700s the period had declined to about 15 years. The mode 2 time series displays more variability over a wider range of timescales than mode 1. However, since the late 1700s, mode 2 has also been dominated by variability in the 60–80-yr range.

8. Summary and conclusions

Our analysis demonstrates that climate variability of the northeast Pacific Ocean over the past 400 years has been dominated by three main periods of oscillation: the well-known interannual (2–8-yr) ENSO cycle, a 20–40-yr interdecadal oscillation, and a 60–80-yr multidecadal oscillation. The ENSO cycle has been the most prominent timescale of the interannual variability in modern climate records for the North Pacific and in high-resolution temperature reconstructions spanning the last 2300 years (Michaelsen 1989; Cook et al. 1995). Recently, Rasmusson et al. (1995) found evidence for a strong century-scale modulation of the amplitude of the ENSO signal based on the observation that the average ENSO event was relatively intense in the late nineteenth century (caused by the very strong 1877, 1888, and 1896 events) and relatively weak between 1920 and 1950 (Table 4). The trend toward more intense El Niño events since 1957 has continued with the strong events in 1983, 1992, and 1997. Rasmusson et al. (1995) also found that the average frequency of the ENSO cycle is modulated, similar to the modulation observed by Michaelsen (1989) and reported here for the air temperature records for Visalia (Fig. 5). Specifically, the average time between ENSO events has been decreasing since the middle of this century. Although it is possible that this change in ENSO return time period could be associated with global warming, we note that reconstructed temperatures along the western margin of North America clearly indicate that ''clusters'' of strong El Niño events have occurred just as frequently (roughly every century) in the past. Therefore, the current increase in the frequency of El Niño events could be largely a continuation of a natural cycle. Gershunov and Barnett (1998) describe a mechanism that might explain this phenomenon. They found that the North Pacific oscillation (NPO) modulates teleconnections in the atmosphere during ENSO events. The high NPO phase is characterized by an anomalously deep Aleutian low, cold western and central North Pacific, and warm eastern Pacific, as well as anomalous warming in the central and eastern tropical Pacific. Reversed climatic condition characterize the low NPO phase. El Niño signals tend to be stronger during the high phase of the NPO, and weaker and spatially incoherent during the low phase of the NPO. This seems to explain why the 1952/53 tropical El Niño (during a low NPO phase) failed to propagate to the two northern sites in our study region, while the 1918, 1925, 1930, 1941, and 1943 events, which occurred during a high NPO phase were strong along the entire west coast of North America (Table 4).

There is growing evidence from both measured and high quality proxy time series data of significant interdecadal variability (20–40-yr timescale) in the North

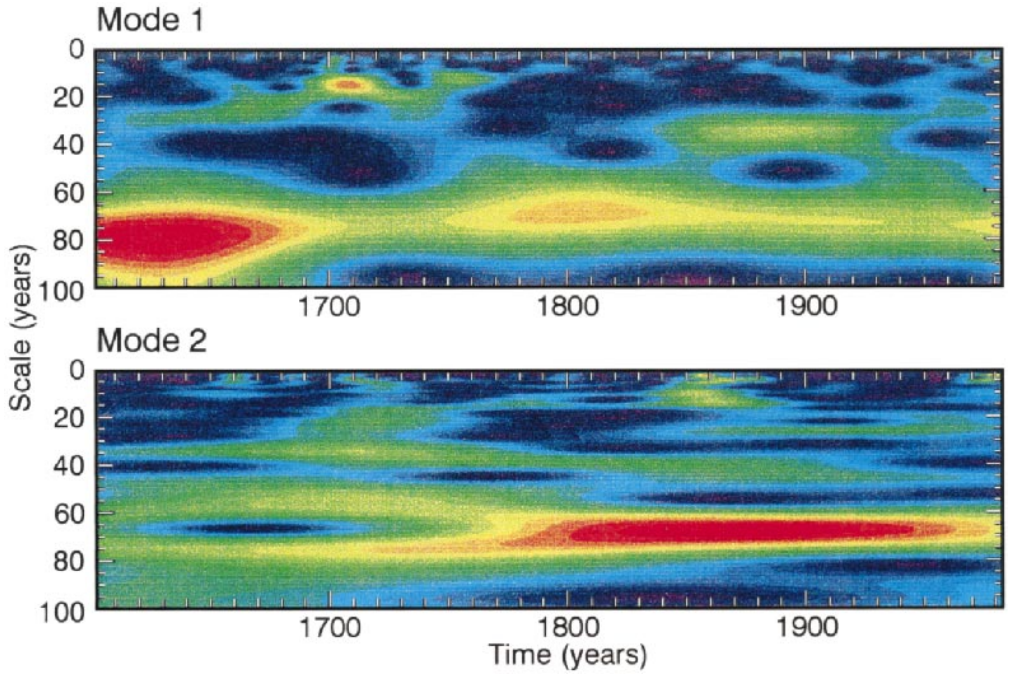

FIG. 9. Time series demodulation of the first and second EOFs. (Top) Mode 1 and (bottom) mode 2. Large signal amplitudes are shown in red and low amplitudes in blue.

Pacific (e.g., Cayan 1980; Royer 1989; Scuderi 1993; Mann et al. 1995; Ware 1995; Mantua et al. 1997; Minobe 1999). Based on state-of-the-art coupled ocean–atmosphere general circulation model simulations, Latif and Barnett (1996) and Yukimoto et al. (1996) suggest possible mechanisms, which could produce quasi-interdecadal oscillations in the North Pacific. White and Cayan (1998) also examined recent interdecadal variability in global ocean sea surface temperature (SST) and sea level pressure (SLP). They found a remarkable periodicity and global symmetry in both the pattern and evolution of the interdecadal SST and SLP climate signals, suggesting that interdecadal variability arises as a worldwide phenomenon relying upon global interactions to account for its existence. They proposed that the equatorward advection of extratropical SST anomalies into tropical regions (in all oceans) and equatorial regions (in some oceans) by the eastern and tropical branches of the subtropical gyre (taking about 10 years) provides the delayed negative feedback mechanism responsible for the periodicity of the decadal variability. This mechanism is presumed to spawn meridional atmospheric teleconnections that reverse extratropical westerly wind anomalies and generate extratropical SST anomalies of opposite sign. Repeating this process yields a delay action oscillator capable of producing the observed, nominal 20-yr cycle in SSTs. Figure 4 suggests that over the last 400 years the period of this interdecadal oscillation in the northeast Pacific has averaged about 35 years. However, in the last half of the twentieth century the period has declined to about 20 years (Fig. 7). Consistent with our findings, a 31-yr spectral peak is also prominent in Scuderi's (1993) analysis of a 2000-yr temperature reconstruction from the same general area as our two southern sites, and in Cook et al.'s (1995) 2300-yr temperature reconstruction for the South Pacific.

There is also evidence of significant climate variability at a 50–80-yr timescale in the North Pacific (Scuderi 1993; Mann et al. 1995; Ware 1995; Minobe 1997). Minobe (1997) analyzed spring air temperature reconstructions derived from tree ring width chronologies (Fritts 1991) from an extensive area in western North America. He found statistically significant peaks between 50- and 70-yr periods, but concluded that this signal was only prevalent from the eighteenth century to the present. Our results are in broad agreement with Minobe's. However, in retrospect, by selecting only tree ring sites that were closest to the coast, and by using the annual air temperature reconstructions, which are slightly more reliable than spring air temperature reconstructions (Fritts and Lough 1985), we have been able to resolve the 60–80-yr signal at all five sites in our study region. Consequently, our results extend Minobe's conclusions, indicating that the nominal 70-yr climate oscillation has been prevalent along the west coast of North America for the last 400 years (at least), and that it is the predominant signal in the subtropical coastal climate south of 40°N. A possible explanation for this phenomenon is suggested in a recent study by Yukimoto et al. (2000), who conducted a 150-yr integration experiment with the Japan Meteorological Re-

search Institute (JMI) GCM. Their preliminary complex EOF analysis of model SST variability yielded spectral peaks around 20 years and a pronounced spectral peak around 75 years. The latter oscillation in SST was strongest in the central and eastern North Pacific and absent in the tropical Pacific. The centers of action of this signal are in the northwest Pacific around the Sea of Okhotsk and in the central North Pacific near Hawaii. These two action centers are 180° out of phase. These preliminary results suggest that there might be a strong meridional variation in the amplitude of the 60–80-yr oscillation with a possible transition taking place somewhere around the latitude of the subtropical convergence, which separates the subarctic and subtropical regions of the North Pacific. This would be consistent with our findings that indicate a strong, persistent 60–80-yr temperature oscillation at the latitude of Southern California, and a generally weaker signal at higher latitudes in the northeast Pacific.

In closing, we note that the 60–80-yr oscillation provides the basic timescale for climate regimes in the North Pacific (Minobe 1997), and that the last regime change occurred around 1976. Since the reconstructed temperature records that we examined indicate that warm regimes along the western margin of North America have lasted on average about 32 years, we concur with Minobe (1999) that the next regime change, toward a cooler climate and less intense Aleutian low pressure distribution in the northeast Pacific, could occur sometime in the current decade.

Acknowledgments. This work was inspired by Michaelsen's 1989 paper. We thank Stephannie Faint for her help, and our Japanese colleagues, Dr. Endoh and Dr. Yukimoto, for sharing their preliminary findings with us. Dr. Badal Pal assisted with the analysis and figure preparation, and Patricia Kimber drafted the final figures. This contribution was funded in part by the Canadian GLOBEC program.

REFERENCES

Cayan, D. R., 1980: Regimes and events in recent climatic variables. *Calif. Coop. Oceanic Fish. Invest. Rep.,* **21,** 90–101.

——, D. R. McLain, W. D. Nichols, and J. S. DiLeo-Stevens, 1991: Monthly climatic time series data for the Pacific Oceans and western Americas. U.S. Geological Survey Open-File Rep. 91–92, 380 pp. [Available from American Geophysical Union, 2000 Florida Ave. NW, Washington, DC 20009.]

Cook, R., B. Buckley, and R. D. Arrigo, 1995: Interdecadal temperature oscillations in the Southern Hemisphere: Evidence from Tasmanian tree rings since 300 B.C. *Natural Climate Variability on Decade-to-Century Time Scales.* D. G. Martinson et al., Eds., National Academy Press, 523–532.

Douglas, A. V., 1980: Geophysical estimates of sea-surface temperatures off western North America since 1671. *Calif. Coop. Oceanic Fish. Invest. Rep.,* **21,** 102–112.

Ebbesmeyer, C. C., D. R. Cayan, D. R. McLain, F. H. Nichols, D. H. Peterson, and K. T. Redmond, 1991: 1976 step in the Pacific climate: Forty environmental changes between 1968 and 1975 and 1977–1984. *Proc. Seventh Annual Pacific Climate (PACLIM) Workshop. Tech. Rep.* 26, Asilomar, CA, California Department of Water Resources, 115–126.

Emery, W. J., and R. E. Thomson, 1998: *Data Analysis Methods in Physical Oceanography.* Pergamon Press, 634 pp.

Fritts, H. C., 1991: *Reconstructing Large-Scale Climatic Patterns from Tree-Ring Data.* University of Arizona Press, 286 pp.

——, and J. M. Lough, 1985: An estimate of the average annual temperature variations for North America, 1602 to 1961. *Climatic Change,* **7,** 203–224.

Gershunov, A., and T. P. Barnett, 1998: Interdecadal modulation of ENSO teleconnections. *Bull. Amer. Meteor. Soc.,* **79,** 2715–2725.

Hsieh, W. W., D. M. Ware, and R. E. Thomson, 1995: Wind-induced upwelling along the west coast of North America, 1899–1988. *Can. J. Fish. Aquat. Sci.,* **52,** 325–334.

Latif, M., and T. Barnett, 1996: Decadal climate variability over the North Pacific and North America: Dynamics and predictability. *J. Climate,* **9,** 2407–2423.

Mann, E. M., J. Park, and R. S. Bradley, 1995: Global interdecadal and century-scale climate oscillations during the past five centuries. *Nature,* **378,** 266–270.

Mantua, N. J., S. R. Hare, Y. Zhang, J. M. Wallace, and R. C. Francis, 1997: A Pacific interdecadal climate oscillation with impacts on salmon production. *Bull. Amer. Meteor. Soc.,* **78,** 1069–1079.

Michaelson, J., 1989: Long-period fluctuations in El Niño amplitude and frequency reconstructed from tree-rings. *Geophys. Monogr.,* No. 55, Amer. Geophys. Union, 69–74.

Minobe, S., 1997: An oscillation of period 50–70 years over the North Pacific. *Geophys. Res. Lett.,* **24,** 683–686.

——, 1999: Resonance in bidecadal and pentadecadal climate oscillations over the North Pacific: Role in climatic regime shifts. *Geophys. Res. Lett.,* **26,** 855–858.

Rasmusson, E. M., X. Wang, and C. F. Ropelewski, 1995: Secular variability of the ENSO cycle. *Natural Climate Variability on Decade-to-Century Time Scales,* D. G. Martinson et al., Eds., National Academy Press, 458–471.

Roden, G. I., 1989: Analysis and interpretation of long-term climatic variability along the west coast of North America. *Geophys. Monogr.,* No. 55, Amer. Geophys. Union, 93–111.

Royer, T. C., 1989: Upper ocean temperature variability in the northeast Pacific Ocean: Is it an indicator of global warming? *J. Geophys. Res.,* **94,** 18 175–18 183.

Schwing, F. B., 1994: Long-term and seasonal patterns in coastal temperature and salinity along the North American west coast. *Proc. Tenth Annual Pacific Climate (PACLIM) Workshop. Tech. Rep.* 36, Asilomar, CA, California Department of Water Resources, 1–15.

Scuderi, L. A., 1993: A 2000-year tree ring record of annual temperatures in the Sierra Nevada mountains. *Science,* **29,** 1433–1436.

Ware, D. M., 1995: A century and a half of change in the climate of the NE Pacific. *Fish. Oceanogr.,* **4,** 267–277.

——, and R. E. Thomson, 1991: Link between long-term variability in upwelling and fish production in the northeast Pacific Ocean. *Can. J. Fish. Aquat. Sci.,* **48,** 2296–2306.

White, W. B., and D. R. Cayan, 1998: Quasi-periodicity and global symmetries in interdecadal upper ocean temperature variability. *J. Geophys. Res.,* **103,** 21 335–21 354.

Yukimoto, S., M. Endoh, Y. Kitamura, A. Kitoh, T. Motoi, A. Noda, and T. Tokioka, 1996: Interannual and interdecadal variabilities in the Pacific in an MRI coupled GCM. *Climate Dyn.,* **12,** 667–683.

——, ——, ——, ——, ——, and ——, 2000: ENSO-like interdecadal variability in the Pacific Ocean as simulated in a coupled general circulation model. *J. Geophys. Res.,* in press.